Preprints of the 19th World Congress
The International Federation of Automatic Control
Cape Town, South Africa. August 24-29, 2014

Nonlinear Robust Visual Servo Control for Robotic Citrus Harvesting

S. S. Mehta * **W. MacKunis** ** **T. F. Burks** ***

* *Department of Industrial and Systems Engineering, University of Florida, Shalimar, FL-32579 (e-mail: siddhart@ufl.edu).*
** *Physical Sciences Department, Embry-Riddle Aeronautical University, Daytona Beach, FL-32114 (e-mail: william.mackunis@erau.edu)*
*** *Department of Agricultural and Biological Engineering, University of Florida, Gainesville, FL-32611 (e-mail: tburks@ufl.edu)*

Abstract: In this paper, a cooperative visual servo controller is presented for autonomous citrus harvesting. A fixed camera provides a global view of a tree canopy for the camera-in-hand, attached to the end-effector, to servo to a target fruit. The paper focuses on the development of a robust, image-based, nonlinear visual servo controller to regulate the end-effector to the fruit location in the presence of unknown fruit motion. A robust feedback term is included in the controller to compensate for the bounded fruit motion, for example, due to wind gusts and robot-tree contact. Lyapunov-based stability analysis guarantees uniformly ultimately bounded regulation of the end-effector. The presented work differs from the existing methods in that the fruit motion in the form of unknown disturbance dynamics are included in the control formulation to actively compensate for the motion without the need for high-frequency image feedback.

Keywords: Robust Control, Robotic Harvesting, Agricultural Robotics, Fruit Motion

1. INTRODUCTION

One of the earliest programs in robotic fruit harvesting worldwide was begun at the University of Florida in the 1980's by Harrell et al. (1990b). Subsequently, numerous researchers around the world studied robotic solutions for fresh market fruit as well as vegetable harvesting. A comprehensive review of robotic systems in agriculture can be found in Tillett (1993); Sarig (1993); Hannan and Burks (2004); Li et al. (2011). According to Sarig (1993), the major problems that must be solved with a robotic picking system include recognizing and locating the fruit, and detaching it according to prescribed criteria, without damaging either the fruit or the tree. In addition, the robotic system needs to be economically sound to warrant its use as an alternative method to hand picking. Ceres et al. (1998) developed an aided fruit harvesting strategy, where an operator performed detection of fruits by means of a laser rangefinder (LRF). The identified position of fruit in spherical coordinates was used to control the three degrees-of-freedom (DOF) manipulator for harvesting. d'Esnon (1985); d'Esnon et al. (1987) developed a vision-based three DOF, hydraulically powered spherical coordinate manipulator - MAGALI - for golden apple harvesting, where a monocular camera detected a fruit during a vertical scan. Subsequently, the telescopic arm translated along the optical beam until it reached the fruit, which was sensed by a photoelectric sensor. Ceres et al. (1998); d'Esnon et al. (1987) relied on open-loop position control, i.e., dead-reckoning, of a robotic manipulator, thus being vulnerable to fruit motion. The Florida Citrus Picking Robot by Harrell et al. (1989, 1990a,b), with the goal of overcoming the limitations of MAGALI, used a closed-loop camera-in-hand (CiH) configuration along with an ultrasound transducer for fruit range identification. Computationally inexpensive contrast-based fruit classification methods used by Harrell et al. can provide high-frequency image feedback that can passively compensate for the fruit motion. However, certain outdoor conditions (e.g., cloudy or bright day) may require sophisticated image processing for efficient classification, thus leaving the system susceptible to fruit motion. Levi et al. (1988) investigated a vision-based cylindrical manipulator system for robotic citrus harvesting. Due to the chosen camera configuration and dead-reckoning during the reaching stage, the harvesting accuracy is susceptible to mechanical backlash, bearing wear, and slippage. In Rabatel et al. (1995); Juste and Sevila (1991), the French and Spanish researchers proposed a robotic citrus harvesting system called EUREKA. A Bayesian classifier detected mature fruit from the grayscale images captured by a monocular vision system. For the spherical manipulator, the robot motion trajectory was along the straight line between the camera optical center and the fruit. Muscato et al. (2005) devel-

⋆ This research is supported in part by a grant from the United States Department of Agriculture Small Business Innovation Research (USDA-SBIR) award contract #2012-00032, the USDA NIFA AFRI National Robotics Initiative #2013-67021-21074, the AFRL Mathematical Modeling and Optimization Institute contract #FA8651-08-D-0108/042, and the ASEE Air Force Summer Faculty Fellowship Program. Any opinions, findings and conclusions or recommendations expressed in this material are those of the author(s) and do not necessarily reflect the views of the funding agency.

oped a citrus harvesting robot prototype called CRAM, where the differential image size of the fruit was used to identify the distance to a fruit, thus, avoiding the need for additional range measurement sensors. However, Muscato et al. (2005) expressed the need for robust and adaptive control methods in robot manipulation. A tomato harvesting robot in greenhouse conditions was presented in Buemi et al. (1996), where a stereo-vision system was employed to servo a six DOF robotic manipulator. Murakami et al. (1999) proposed a vision-based robotic cabbage harvester utilizing neural network-based image processing for target detection. The vision-based cabbage harvesting problem was reduced to a 2D visual servo control problem, where a template matching approach was used to determine the location and diameter of cabbage for robot manipulation. Hayashi et al. (2002) studied the development of a robotic harvesting system for eggplants. An articulated five DOF manipulator in CiH configuration with a fuzzy logic-based visual servo controller was presented for eggplant harvesting. A tomato, petty-tomato, cucumber, and grape harvesting robot was studied by Kondo et al. (1996) in Japan; a seven DOF, kinematically redundant tomato harvesting robot exhibited a stereo-vision system for depth estimation. A vision-based robotic cucumber harvesting system was investigated by Van Henten et al. (2002, 2003). The vision system consisted of a fixed camera and a CiH; the fixed camera was used for collision-free motion planning, while the CiH located the fruit by triangulation using the known robot motion.

Previous research at large focused on the development of robotic manipulators, end-effectors, and suitable target classification methods. Although the need is expressed in the literature, relatively little or no attention has been paid to robust control formulation and rigorous stability analysis of harvesting systems. Exogenous disturbances, such as wind gusts and robot-tree contact, may cause an unknown time-varying fruit motion that can result in lower harvesting efficiency. Closed-loop systems relying on disturbance compensation using high-frequency feedback (Harrell et al., 1989, 1990a,b) alone can be susceptible to large positioning errors as disturbance dynamics are not taken into account while developing the control system. Moreover, computationally demanding image processing methods required for improved fruit detection can restrict the feedback frequency for real-time implementations. Advances in control systems theory can be exploited to allow efficient use of the existing hardware and high-fidelity image processing methods by designing a robust controller to solve the unknown fruit motion problem. In this paper, a robust visual servo controller is developed, where a robust feedback element introduced in the control law compensates for an unmodeled, non-vanishing, nonlinear disturbance. A Lyapunov-based nonlinear controller and rigorous stability analysis is presented, which guarantees uniformly ultimately bounded regulation of the robot end-effector. To the best knowledge of the authors, the presented work is the first to provide a robust nonlinear controller formulation and detailed stability analysis for robotic fruit harvesting. The developed robust, image-based nonlinear translation controller regulates the end-effector to the actual fruit location, even in the presence of fruit motion.

2. EUCLIDEAN RECONSTRUCTION

Consider the orthogonal coordinate frames $\mathcal{F}$, $\mathcal{F}_f$, and $\mathcal{F}_b$ as shown in Figure 1. The time-varying coordinate frame $\mathcal{F}$ is attached to a CiH, *i.e.*, a camera held by a robot end-effector. The coordinate frame $\mathcal{F}_f$ is attached to a fixed camera, for example, a stationary camera mounted in the workspace of a robot; and the coordinate frame $\mathcal{F}_b$ is attached to the stationary base of a robot. The unknown Euclidean coordinates of the fruit center, $\bar{m}(t), \bar{m}_f \in \mathbb{R}^3$, expressed in terms of $\mathcal{F}$ and $\mathcal{F}_f$, respectively, are given as

$$\bar{m}(t) = \left[\, x(t) \;\; y(t) \;\; z(t) \,\right]^T, \quad \bar{m}_f = \left[\, x_f \;\; y_f \;\; z_f \,\right]^T \tag{1}$$

where $z(t), z_f \in \mathbb{R}$ denote the unknown depth of the target fruit measured in $\mathcal{F}$ and $\mathcal{F}_f$, respectively. The Euclidean-

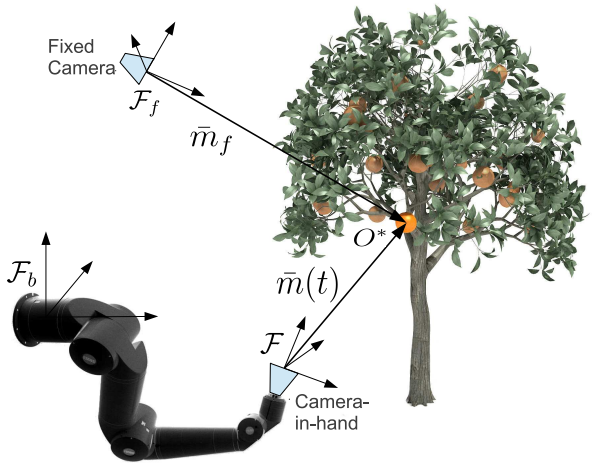

Fig. 1. Coordinate frame relationships, where the time-varying frame $\mathcal{F}$ is attached to the camera-in-hand, $\mathcal{F}_f$ corresponds to the fixed camera, and $\mathcal{F}_b$ is attached to the stationary base of the robot.

space is projected onto the image-space, and $m(t)$ and m_f denote the corresponding normalized Euclidean coordinates of the fruit center as

$$m(t) = \left[\frac{x(t)}{z(t)} \;\; \frac{y(t)}{z(t)} \;\; 1 \right]^T, \quad m_f = \left[\frac{x_f}{z_f} \;\; \frac{y_f}{z_f} \;\; 1 \right]^T. \tag{2}$$

Assumption 1. In (2), it is assumed that the unknown depths $z(t), z_f \geq \varepsilon$, where $\varepsilon \in \mathbb{R}_{>0}$ is an arbitrary constant. This is a standard assumption in visual servo control, which physically means that the target is always in front of the camera.

In addition to having normalized Euclidean coordinates, the target point will also have pixel coordinates acquired by the CiH and the fixed camera. Let $p(t), p_f \in \mathbb{R}^2$ denote the pixel coordinates of the target center expressed in $\mathcal{F}$ and $\mathcal{F}_f$, respectively, as

$$p(t) \triangleq \left[\, u(t) \;\; v(t) \,\right]^T, \qquad p_f \triangleq \left[\, u_f \;\; v_f \,\right]^T. \tag{3}$$

Since the normalized Euclidean coordinates in (2) cannot be measured directly, a global invertible transformation (i.e., the pinhole camera model) is used to determine the normalized Euclidean coordinates from the corresponding pixel information as

$$\left[\, p^T \;\; 1 \,\right]^T = Am, \qquad \left[\, p_f^T \;\; 1 \,\right]^T = A_f m_f. \tag{4}$$

In (4), $A, A_f \in \mathbb{R}^{3\times3}$ denote the known constant invertible intrinsic camera calibration matrices for the CiH and the fixed camera, respectively.

The depth estimation method presented in Mehta and Burks (2014) along with (2) can be used to obtain the estimated fruit position in $\mathcal{F}_f$ as $\hat{\bar{m}}_f \in \mathbb{R}^3$. Using the extrinsic calibration parameters for the fixed camera and the robot forward kinematics, the estimated position $\hat{\bar{m}}_f$ expressed in $\mathcal{F}_b$ and $\mathcal{F}$ be denoted by $\hat{\bar{m}}_b, \hat{\bar{m}}'(t) \in \mathbb{R}^3$, respectively.

Remark 1. When a fruit is visible to the CiH, the time-varying depth $\hat{z}(t)$ and position $\hat{\bar{m}}(t) \in \mathbb{R}^3$ of the fruit with respect to $\mathcal{F}$ can be obtained. It can be shown that the unknown depth ratio $\hat{z}/z$ denoted by $\xi \in \mathbb{R}_{>0}$ is constant.

3. CONTROL OBJECTIVE

The objective is to locate the robot end-effector to the target fruit for harvesting in the presence of unknown fruit motion. The control objective can be achieved by regulating the time-varying fruit pixel coordinates $p(t)$ to the desired image coordinates, and regulating the end-effector to the desired fruit depth. Hence, mathematically, the control objective can be stated as

$$p(t) \to p_d,\ p_d = [\, u_0 \ v_0 \,]^T \text{ and } z(t) \le z_d \tag{5}$$

where $z_d \in \mathbb{R}_{>0}$ denotes the maximum desired depth of the fruit in $\mathcal{F}$, and $u_0, v_0 \in \mathbb{R}$ denote the pixel coordinates of the principal point (i.e., the intersection of an optical axis with the image plane) of the CiH.

The actual kinematic control inputs for the robot can be obtained from the subsequently developed camera control velocities using a relationship that depends on the extrinsic calibration parameters as (Malis and Chaumette (2002))

$$\begin{bmatrix} v_c \\ \omega_c \end{bmatrix} = \begin{bmatrix} R_e & [t_e]_\times R_e \\ \mathbf{0} & R_e \end{bmatrix} \begin{bmatrix} v_r \\ \omega_r \end{bmatrix} \tag{6}$$

where $v_c(t),\ \omega_c(t) \in \mathbb{R}^3$ denote the linear and angular velocity of the camera; $v_r(t),\ \omega_r(t) \in \mathbb{R}^3$ denote the linear and angular velocity of the robot; $R_e \in \mathbb{R}^{3\times3}$ denotes the known constant rotation between the CiH and robot end-effector frames; and $[t_e]_\times \in \mathbb{R}^{3\times3}$ is the skew symmetric matrix of $t_e \in \mathbb{R}^3$, which denotes the known constant translation vector between the CiH and robot frames.

4. CONTROLLER DEVELOPMENT

Based on the control objective in Section 3, a decoupled rotation and nonlinear image-based translation controller is developed in this section. The fixed camera can view an entire tree canopy and select a fruit to be harvested. However, the target fruit selected by the fixed camera may not be visible to the CiH; therefore, the CiH needs to be oriented along the target fruit. Following the orientation, the CiH is regulated to the desired fruit position using an image-based translation controller. The presented control development assumes an external nonlinear disturbance, such as wind gust and robot-tree contact, to act on the target fruit causing unknown fruit motion.

4.1 Rotation Controller

In this section, a controller is developed to orient the robot end-effector such that the target fruit enters the FOV of the CiH. The rotation error $e_\omega(t) \in \mathbb{R}^3$, which is defined as the orientation mismatch that brings the target fruit into the FOV of the CiH, can be expressed in terms of an angle-axis representation as

$$e_\omega \triangleq u\theta \tag{7}$$

where $u(t) \in \mathbb{R}^3$ represents a unit axis of rotation such that $u(t) = \overrightarrow{\hat{\bar{m}}'}(t) \wedge [\,0\ 0\ 1\,]^T$, and $\theta(t) = \cos^{-1}\langle \overrightarrow{\hat{\bar{m}}'}(t), [\,0\ 0\ 1\,]^T \rangle$, $\theta(t) \in \mathbb{R}$ is the angle of rotation about $u(t)$ such that $0 \le \theta(t) \le \pi$. $\overrightarrow{\hat{\bar{m}}'}(t) \in \mathbb{R}^3$ represents a unit vector along $\hat{\bar{m}}'(t)$. A globally asymptotically stable rotation control input $\omega_c = -k_\omega e_\omega$ can be developed, where $k_\omega \in \mathbb{R}_{>0}$ is a constant control gain (For proof, see Malis and Chaumette (2002) and Mehta and Burks (2014)).

4.2 Translation Controller

Taking the time derivative of (4), the velocity of the CiH can be related to the velocity $\dot{p}(t) \in \mathbb{R}^2$ of the feature point in the image plane of the CiH as

$$\dot{p} = \begin{bmatrix} \dot{u} \\ \dot{v} \end{bmatrix} = -\frac{1}{z} J_v v_c - J_\omega \omega_c + \frac{1}{z} J_v v_d. \tag{8}$$

In (8), $J_v(u,v), J_\omega(u,v) \in \mathbb{R}^{2\times3}$ are the measurable image Jacobians that relate the linear and angular velocity, $v_c(t)$ and $\omega_c(t)$, respectively, of the CiH and the unknown fruit velocity $v_d(t) \in \mathbb{R}^3$ to the fruit image velocity. The fruit is considered a point mass, and the velocity $v_d(t)$ is due to exogenous disturbances acting on the fruit.

Since no orientation change is required during translation control, the image dynamics for translation control can be obtained by substituting $\omega_c(t) = 0$ in (8) as

$$\dot{p} = -\frac{1}{z} J'_v v'_c - \frac{1}{z} J''_v v_{cz} + \frac{1}{z} J'_v v'_d + \frac{1}{z} J''_v v_{dz} \tag{9}$$

where $v_{cz}(t), v_{dz}(t) \in \mathbb{R}$ is the control velocity and the unknown fruit velocity along the optical axis of the camera, respectively. In (9), $J'_v \in \mathbb{R}^{2\times2}$ and $J''_v(u,v) \in \mathbb{R}^2$ are the measurable Jacobians, and $v'_c(t), v'_d(t) \in \mathbb{R}^2$ is the control velocity and the unknown fruit velocity along the image x and y-axis, respectively, given by

$$J'_v = \begin{bmatrix} \lambda_x f & 0 \\ 0 & \lambda_y f \end{bmatrix} \quad J''_v = -\begin{bmatrix} u \\ v \end{bmatrix} \quad v'_c = \begin{bmatrix} v_{cx} \\ v_{cy} \end{bmatrix}. \tag{10}$$

The unknown fruit velocities $v'_d(t)$ and $v_{dz}(t)$ in (9) satisfy $\|v'_d(t)\| \le \gamma_p$ and $\|v_{dz}(t)\| \le \gamma_z$ where $\gamma_p, \gamma_z \in \mathbb{R}_{>0}$ are the known bounding constants. Since an external disturbance such as wind gust will not cause unbounded fruit velocities the above assumption is valid.

Based on the control objective in (5), the translation error $e_v(t) = [e_{v1}(t)\ e_{v2}(t)]^T \in \mathbb{R}^3$ can be defined as

$$e_{v1} \triangleq p - p_d \tag{11}$$

$$e_{v2} \triangleq \alpha\hat{z} - z_d \tag{12}$$

where $\alpha \in \mathbb{R}_{>0}$ is an arbitrarily chosen constant that ensures $\alpha\hat{z} \ge z$. Taking the time-derivative of (12), and using the depth ratio ξ defined in Remark 1, the open-loop error dynamics can be obtained as

$$\dot{e}_{v2} = -\alpha\xi v_{cz} + v_{dz}. \tag{13}$$

Based on (13), the linear velocity $v_{cz}(t)$ of the CiH along the optical axis is designed as

$$v_{cz} = k_z e_{v2} + \frac{e_{v2}\gamma_z^2}{|e_{v2}|\gamma_z + \epsilon_z} - w\|e_{v1}\|^2 \tag{14}$$

where $k_z = k_{z1} + k_{z2} \in \mathbb{R}_{>0}$ is a constant control gain, $\epsilon_z \in \mathbb{R}_{>0}$ is an arbitrarily small design constant, and $w \in \mathbb{R}_{>0}$ is a user defined weight on term $\|e_{v1}\|^2$. The second term in (14) represents a disturbance-rejecting robust feedback term. Substituting (14) into (13), the closed-loop error system can be obtained as

$$\dot{e}_{v2} = -\alpha\xi k_z e_{v2} - \frac{\alpha\xi e_{v2}\gamma_z^2}{|e_{v2}|\gamma_z + \epsilon_z} + v_{dz} + \alpha\xi w\|e_{v1}\|^2. \tag{15}$$

Remark 2. From Remark 1 and the definition of α in (12), the product $\alpha\xi \geq 1$. Therefore, the closed-loop system in (15) is a stable linear system (for proof, see Section 5) subjected to an additive disturbance $\alpha\xi w\|e_{v1}\|^2$, such that if $e_{v1}(t) \in \mathcal{L}_\infty$ then $e_{v2}(t) \in \mathcal{L}_\infty$. The added disturbance $\alpha\xi w\|e_{v1}\|^2$ guarantees that the target fruit is centered in the CiH FOV before reaching the fruit.

After taking the time-derivative of (11) and substituting (9) into the resulting expression, the open-loop error system can be obtained as

$$\dot{e}_{v1} = -\frac{1}{z}J_v' v_c' - \frac{1}{z}J_v'' v_{cz} + \frac{1}{z}J_v' v_d' + \frac{1}{z}J_v'' v_{dz}. \tag{16}$$

Based on the open-loop error system in (16) and the subsequent stability analysis, the linear control velocity $v_c'(t) \in \mathbb{R}^2$ of the CiH can be designed as

$$v_c'(t) = J_v'^{-1}\left((\alpha\hat{z}k_p + \gamma_z)\, e_{v1} - J_v'' v_{cz} + \frac{\|J_v'\| e_{v1}\gamma_p^2}{\|e_{v1}\|\gamma_p + \epsilon_p} + \frac{\|p_d\| e_{v1}\gamma_z^2}{\|e_{v1}\|\gamma_z + \epsilon_{\bar{z}}}\right) \tag{17}$$

where $k_p \in \mathbb{R}_{>0}$ is a constant control gain, and $\epsilon_p, \epsilon_{\bar{z}} \in \mathbb{R}_{>0}$ are arbitrarily small design constants. The last two bracketed entries in (17) are the robust feedback terms. After substituting the control input in (17) into (16), and using $\hat{z}/z = \xi$, the closed-loop error system can be obtained as

$$\dot{e}_{v1} = -\left(\alpha\xi k_p + \frac{\gamma_z}{z}\right) e_{v1} - \frac{\|J_v'\| e_{v1}\gamma_p^2}{z\left(\|e_{v1}\|\gamma_p + \epsilon_p\right)} + \frac{1}{z}J_v' v_d' - \frac{\|p_d\| e_{v1}\gamma_z^2}{z\left(\|e_{v1}\|\gamma_z + \epsilon_{\bar{z}}\right)} - \frac{1}{z}\left(e_{v1} + p_d\right) v_{dz} \tag{18}$$

where the fact that $J_v'' = -p$ along with (11) is used.

5. STABILITY ANALYSIS

Theorem 1. The translation control inputs developed in (14) and (17) ensure uniformly ultimately bounded target fruit regulation in the sense that

$$\|e_{v1}(t)\|^2 \leq \zeta_0 \exp\{-\zeta_1 t\} + \zeta_2 \tag{19}$$

$$\|e_{v2}(t)\|^2 \leq \zeta_3 \exp\{-\zeta_4 t\} + \zeta_5 \tag{20}$$

where ζ_0, ζ_1, ζ_2, ζ_3, ζ_4, $\zeta_5 \in \mathbb{R}$ denote positive bounding constants.

Proof 1. Let $V_1(t)$ be the following nonnegative function:

$$V_1 = \frac{1}{2}e_{v1}^T e_{v1} \tag{21}$$

$$\lambda_1\|e_{v1}\|^2 \leq V_1 \leq \lambda_2\|e_{v1}\|^2 \tag{22}$$

where $\lambda_1, \lambda_2 \in \mathbb{R}_{>0}$ are known bounding constants. Taking the time-derivative of $V_1(t)$ and using (18), the upper bound on the Lyapunov derivative can be obtained after canceling the common terms as

$$\dot{V}_1 \leq -\alpha\xi k_p\|e_{v1}\|^2 - \frac{\|p_d\|\|e_{v1}\|^2\gamma_z^2}{z\left(\|e_{v1}\|\gamma_z + \epsilon_{\bar{z}}\right)} - \frac{\|J_v'\|\|e_{v1}\|^2\gamma_p^2}{z\left(\|e_{v1}\|\gamma_p + \epsilon_p\right)} + \frac{\|p_d\|\|e_{v1}\|\gamma_z}{z} + \frac{\|J_v'\|\|e_{v1}\|\gamma_p}{z} \tag{23}$$

where the facts that $\|v_d'(t)\| \leq \gamma_p, \|v_{dz}(t)\| \leq \gamma_z$ are used. The expression in (23) can be simplified as

$$\dot{V}_1 \leq -\alpha\xi k_p\|e_{v1}\|^2 + \frac{\epsilon_p\|J_v'\|}{z} + \frac{\epsilon_{\bar{z}}\|p_d\|}{z}. \tag{24}$$

Consequently, (22) can be used to obtain the inequality

$$\dot{V}_1 \leq -\frac{\alpha\xi k_p}{\lambda_2}V_1 + \epsilon_{\bar{p}} \tag{25}$$

where the inequality $z(t) \geq \epsilon$ in Assumption 1 is used. In (25), $\epsilon_{\bar{p}} \in \mathbb{R}$ is a linear combination of design constants ϵ_p and $\epsilon_{\bar{z}}$. The linear differential inequality in (25) can be solved as

$$V_1 \leq V_1(0)\exp\left\{\frac{-\alpha\xi k_p}{\lambda_2}t\right\} + \frac{\epsilon_{\bar{p}}\lambda_2}{\alpha\xi k_p}\left(1 - \exp\left\{\frac{-\alpha\xi k_p}{\lambda_2}t\right\}\right). \tag{26}$$

The expressions in (21), (22), and (25) can be used to conclude that $e_{v1}(t) \in \mathcal{L}_\infty$. Since $d_p(t) \in \mathcal{L}_\infty$, (18) can be used to conclude that $\dot{e}_{v1}(t) \in \mathcal{L}_\infty$. The inequalities in (22) and (26) can be used to conclude that

$$\|e_{v1}\|^2 \leq \left(\frac{\lambda_2\|e_{v1}(0)\|^2}{\lambda_1} - \frac{\epsilon_{\bar{p}}\lambda_2}{\alpha\xi k_p}\right)\exp\left\{\frac{-\alpha\xi k_p}{\lambda_2}t\right\} + \left(\frac{\epsilon_{\bar{p}}\lambda_2}{\alpha\xi k_p}\right) < \gamma_1\|e_{v1}(0)\| \tag{27}$$

where $\gamma_1 \in \mathbb{R}_{>0}$ is a constant. The result in (19) can now be directly obtained from (27). Hence, the image coordinates of the fruit centroid are regulated within a small region centered at p_d, where the size of the error ball can be reduced by arbitrarily reducing ϵ_p and $\epsilon_{\bar{z}}$.

Using the result in (19), the disturbance term $\alpha\xi w\|e_{v1}\|^2$ in (15) can be upper bounded as $\alpha\xi w\|e_{v1}\|^2 \leq \alpha\xi w(\zeta_0 + \zeta_2)$. To analyze the stability of the closed-loop system (15), consider a positive definite Lyapunov function $V_2(t)$ as

$$V_2 = \frac{1}{2}e_{v2}^2 \tag{28}$$

$$\lambda_3 e_{v2}^2 \leq V_2 \leq \lambda_4 e_{v2}^2 \tag{29}$$

where $\lambda_3, \lambda_4 \in \mathbb{R}_{>0}$ are known bounding constants. Taking the time-derivative of $V_2(t)$ and using (15) and (19), the Lyapunov derivative can be upper bounded as

$$\dot{V}_2 \leq \left(-\alpha\xi k_z|e_{v2}|^2 + \alpha\xi w(\zeta_0 + \zeta_2)|e_{v2}|\right) + \epsilon_z \tag{30}$$

where the fact that $\alpha\xi \geq 1$ is used, i.e., the robust feedback term dominates the unknown disturbance. Completing the squares on the bracketed terms and using (29) yields the following inequality:

$$\dot{V}_2 \leq \frac{-\alpha\xi k_{z1}}{\lambda_4}V_2 + \frac{\alpha\xi w^2(\zeta_0 + \zeta_2)^2}{4k_{z2}} + \epsilon_z. \tag{31}$$

The solution of the linear inequality in (31) is given by

$$V_2 \leq V_2(0)\exp\left\{\frac{-\alpha\xi k_{z1}}{\lambda_4}t\right\} + \frac{\lambda_4}{\alpha\xi k_{z1}}\left(\frac{\alpha\xi w^2(\zeta_0+\zeta_2)^2}{4k_{z2}} + \epsilon_z\right) \times \left(1-\exp\left\{\frac{-\alpha\xi k_{z1}}{\lambda_4}t\right\}\right). \quad (32)$$

From (28), (29), and (31), $e_{v2}(t) \in \mathcal{L}_\infty$. Using the fact that $e_{v1}(t), e_{v2}(t), d_z(t) \in \mathcal{L}_\infty$, the control inputs $v_{cz}(t), v_c'(t) \in \mathcal{L}_\infty$ and closed-loop error system $\dot{e}_{v2}(t) \in \mathcal{L}_\infty$. Therefore, the inequalities in (29) and (32) can be used to conclude that

$$\|e_{v2}\|^2 \leq \left(\frac{\lambda_4\|e_{v2}(0)\|^2}{\lambda_3} - \frac{\lambda_4}{\alpha\xi k_{z1}}\left(\frac{\alpha\xi w^2(\zeta_0+\zeta_2)^2}{4k_{z2}}+\epsilon_z\right)\right) \times \exp\left\{\frac{-\alpha\xi k_{z1}}{\lambda_4}t\right\} + \left(\frac{\alpha\xi w^2(\zeta_0+\zeta_2)^2}{4k_{z2}}+\epsilon_z\right) < \gamma_2|e_{v2}(0)| \quad (33)$$

where $\gamma_2 \in \mathbb{R}_{>0}$ is a constant. The result in (20) follows directly from (33). The translation error $e_{v2}(t)$ along the camera optical axis can be reduced by arbitrarily reducing ϵ_z, hence the end-effector is regulated to the fruit such that $z(t) \leq z_d$. An infrared proximity switch on the end-effector can detect the presence of fruit to stop the manipulator to ensure $\epsilon \leq z(t) \leq z_d$.

6. SIMULATION RESULTS

A numerical simulation was performed to demonstrate the performance of the proposed robust controller for citrus harvesting. The initial position $t_r \in \mathbb{R}^3$ and orientation $R_r \in \mathbb{R}^{3\times3}$ of the CiH coordinate frame $\mathcal{F}$ with respect to $\mathcal{F}_b$ was considered to be

$$t_r = [\,20\;\;60\;\;1500\,]^T,\;\; R_r = \begin{bmatrix} 0.4698 & -0.1955 & 0.8608 \\ 0.1710 & 0.9769 & 0.1285 \\ -0.8660 & 0.0868 & 0.4924 \end{bmatrix}. \quad (34)$$

The unperturbed position of the target fruit in $\mathcal{F}_b$ was assumed to be $O^* = [500\;\;400\;\;2500]^T$. A non-vanishing disturbance is assumed to perturb the fruit with a velocity given by

$$v_d(t) = \frac{d}{dt}[\,20\cos(\theta_p)\sin(\theta_z)\;\;20\sin(\theta_p)\sin(\theta_z)\;\;20\cos(\theta_z)\,]^T$$
$$\theta_p(t) = 60\cos(1.2t) \quad \theta_z(t) = 20\cos(1.2t) \quad (35)$$

The fruit pixel coordinates were also assumed to be affected by a zero-mean Gaussian sensor noise of standard deviation of 1 pixel. Fig. 2 shows the time-varying image-space trajectory of the fruit in the CiH during the rotation (dotted line) and translation control (continuous line). The fruit pixel coordinates are regulated to the center of the CiH so that the fruit can be harvested. The rotation and translation error plots are shown in Figs. 3 and 4, respectively. It can be seen from Fig. 3 that the rotation error vanishes asymptotically while the translation errors, e_{v1} and e_{v2}, in Fig. 4 are bounded even in the presence of unknown disturbances. Figs. 5 and 6 show the angular and linear velocity of the CiH. The control velocities in Figs. 5 and 6 are bounded at all times. It can be seen that for the presented simulation scenario, the fruit can be reached in less than 8s in the presence of unknown fruit motion.

7. CONCLUSION

An image-based nonlinear visual servo controller is presented, where a robust feedback term compensates for the unknown bounded fruit motion due to wind gust or robot-tree contact. In contrast to existing methods, the fruit motion is actively compensated by including disturbance dynamics in the control formulation. A Lyapunov-based stability analysis proves uniformly ultimately bounded regulation of the end-effector. The future work will focus on experimental validation of the developed controller on a kinematically redundant manipulator in field conditions.

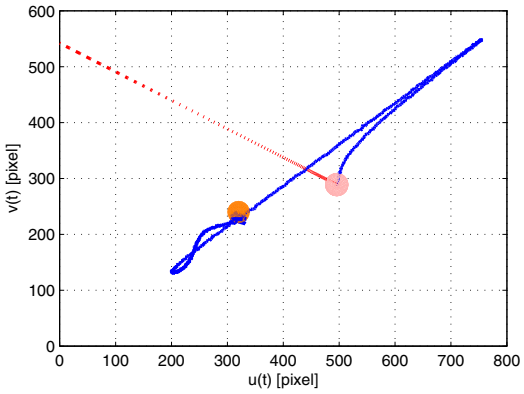

Fig. 2. Image-space trajectory of the target fruit in the CiH during the rotation (dotted line) and translation control (continuous line).

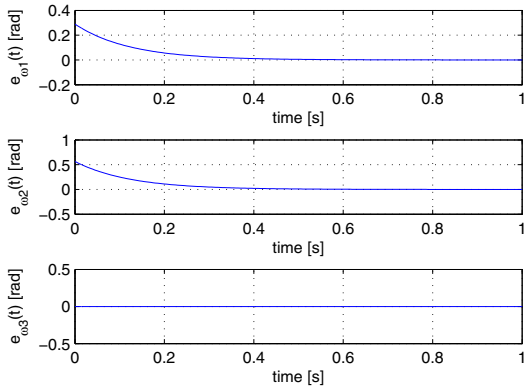

Fig. 3. Rotation error $e_\omega(t) = [e_{\omega1}(t)\;\;e_{\omega2}(t)\;\;e_{\omega3}(t)]^T$.

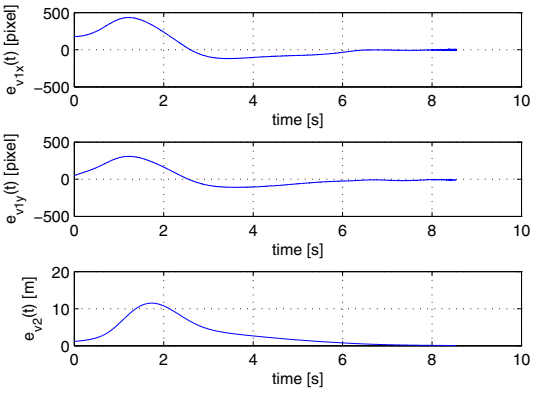

Fig. 4. Translation error $e_v(t) = [e_{v1}^T(t)\;\;e_{v2}(t)]^T$, where $e_{v1}(t) = [e_{v1x}(t)\;\;e_{v1y}(t)]^T$.

REFERENCES

F. Buemi, M. Massa, G. Sandini, and G. Costi. The agrobot project. *Advances in Space Research*, 18(1):

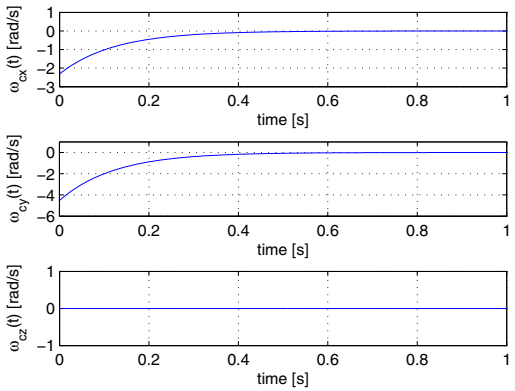

Fig. 5. Angular velocity $\omega_c(t) = [\omega_{cx}(t)\ \omega_{cy}(t)\ \omega_{cz}(t)]^T$.

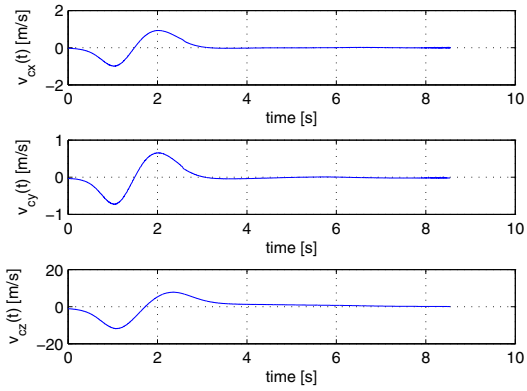

Fig. 6. Linear velocity $v_c(t) = [v_{cx}(t)\ v_{cy}(t)\ v_{cz}(t)]^T$.

185–189, 1996.

R. Ceres, F. L. Pons, A. R. Jimenez, F. M. Martin, and L. Calderon. Design and implementation of an aided fruit-harvesting robot (Agribot). *Industrial Robot*, 25: 337–346, 1998.

A. Grand d'Esnon. Robotic harvesting of apples. In *Agri-Mation 1*, pages 25–28, Chicago, IL, Feb 1985. ASAE.

A. Grand d'Esnon, G. Rabatel, R. Pellenc, A. Journeau, and M. J. Aldon. MAGALI: A self-propelled robot to pick apples. In *Proceedings of American Society of Agricultural Engineers*, pages ASAE Paper. No. 87–1037, Baltimore, Maryland, 1987.

M. W. Hannan and T. F Burks. Current developments in automated citrus harvesting. In *ASABE Annual International Meeting*, page ASAE Paper. No. 043087, 2004.

R. C. Harrell, D. C. Slaughter, and P. D. Adsit. A fruit-tracking system for robotic harvesting. *Machine Vision and Applications*, 2(2):69–80, 1989.

R. C. Harrell, P. D. Adsit, R. D. Munilla, and D. C. Slaughter. Robotic picking of citrus. *Robotica*, 8(04): 269–278, 1990a.

R. C. Harrell, P. D. Adsit, T. A. Pool, R. Hoffman, et al. The Florida robotic grove-lab. *Transactions of the ASAE*, 33(2):391–399, 1990b.

S. Hayashi, K. Ganno, Y. Ishii, and I. Tanaka. Robotic harvesting system for eggplants. *Japan Agricultural Research Quarterly*, 36:163–168, 2002.

F. Juste and F. Sevila. Citrus: an European project to study the robotic harvesting of oranges. In *2nd workshop on robotics in agriculture and food in industry*, pages 187–196, 1991.

N. Kondo, Y. Nishitsuji, P. Ling, and K.C. Ting. Visual feedback guided robotic cherry tomato harvesting. *Transactions of the ASAE*, 39(6):2331–2338, 1996.

P. Levi, A. Falla, and R. Pappalardo. Image controlled robotics applied to citrus fruit harvesting. In *7th International Conference on Robot Vision and Sensory Controls*, Zurich, Switzerland, 1988. IFS Publications.

P. Li, S. Lee, and H. Hsu. Review on fruit harvesting method for potential use of automatic fruit harvesting systems. *Procedia Engineering*, 23:351–366, 2011.

E. Malis and F. Chaumette. Theoretical improvements in the stability analysis of a new class of model-free visual servoing methods. *Robotics and Automation, IEEE Transactions on*, 18(2):176–186, Apr. 2002.

S. S. Mehta and T. F. Burks. Vision-based control of robotic manipulator for citrus harvesting. *Computers and Electronics in Agriculture*, 102:146–158, 2014.

N. Murakami, K. Otsuka, K. Inoue, and M. Sugimoto. Development of robotic cabbage harvester (part 1) - operational speed of the designed robot. *Journal of the Japanese Society of Agricultural Machinery*, 61(5):85–92, 1999.

G. Muscato, M. Prestifilippo, N. Abbate, and I. Rizzuto. A prototype of an orange picking robot: past history, the new robot and experimental results. *Industrial Robot: An International Journal*, 32(2):128–138, 2005.

G. Rabatel, A. Bourely, F. Sevila, and F. Juste. Robotic harvesting of citrus: State-of-art and development of the French Spanish EUREKA project. In *Proceedings of International conference on Harvest and Post harvest Technologies for Fresh Fruits and Vegetables*, pages 232–239, 1995.

Y. Sarig. Robotics of fruit harvesting: A state-of-the-art review. *Journal of Agriculture Enginnering*, 54:265–280, 1993.

N. D. Tillett. Robotic manipulators in horticulture: a review. *Journal of agricultural engineering research*, 55 (2):89–105, 1993.

E. J. Van Henten, J. Hemming, B. A. J. Van Tuijl, J. G. Kornet, J. Meuleman, J. Bontsema, and E. A. Van Os. An autonomous robot for harvesting cucumbers in greenhouses. *Autonomous Robots*, 13(3):241–258, 2002.

E. J. Van Henten, J. Hemming, B. A. J. Van Tuijl, J. G. Kornet, and J. Bontsema. Collision-free motion planning for a cucumber picking robot. *Biosystems Engineering*, 86(2):135–144, 2003.